14th Australasian Fluid Mechanics Conference
Adelaide University, Adelaide, Australia
10-14 December 2001

Prediction of Yacht Roll Motion at Zero Forward Speed

K. Klaka[1] , J. Krokstad[1] and M.R. Renilson[2]

[1]Centre for Marine Science and Technology
Curtin University of Technology, Perth, Western Australia, 6102 AUSTRALIA

[2] Formerly Dept. of Naval Architecture and Ocean Engineering
Australian Maritime College, Launceston, Tasmania, 7250 AUSTRALIA. Now at QinetiQ, UK

Abstract

The roll motion of a yacht at zero Froude number is being investigated, motivated by limitations of existing theoretical models of roll motion when applied to bodies with large appendages. A time domain single degree of freedom roll model has been developed in order to identify the dominant excitation and damping sources. The canoe body forces were determined from a wave diffraction program whilst the appendages were treated as fully submerged flat plates. Calculation of the forces acting was based on a stripwise Morison formulation. A series of full scale validation experiments has also been conducted, in calm water and in ocean waves.

The results show that the keel, rudder and sail dominate the damping, whilst the canoe body contributes very little. The hydrodynamic damping was non-linear with respect to wave amplitude, but the overall damping with a sail hoisted is only weakly non-linear with respect to wave amplitude because the sail dominates the damping, particularly in a wind field. The numerical model predicts a strong influence of wave heading which is not borne out by the full scale trials.

Introduction

The roll motion of a yacht at zero Froude number is being investigated. The objectives of the research are to:

- Predict the roll motion of a vessel at zero ship speed in a low amplitude ocean wave field, over a range of headings.
- Estimate the influence of wind direction, wind speed, ocean current and anchor tether forces on roll at zero ship speed.

Viscous forces on the appendages are important and the non-linear nature of roll response requires time domain modelling [1], [2].

As a preliminary step, a series of full scale experiments were conducted on a sailing yacht in calm water and in multi-directional ocean waves. Then a time domain single degree of freedom roll model was written. The canoe body forces were determined from a wave diffraction program. The appendages were treated as fully submerged flat plates and calculation of the forces acting was based on a stripwise Morison formulation [3].

Numerical Model

The model received linear input from a sinusoidal wave field and used frequency-dependent coefficients for several of the force terms. The resulting motions output was non-linear with respect to wave amplitude. The canoe body and the appendage forces were treated separately.

Underlying assumptions included:

- zero vessel forward speed;
- infinite water depth;
- appendages treated as flat plates with no free-surface effects;
- the roll axis and vertical centre of gravity fixed at the design waterline.

The hull force model is described in Figure 1. Output from a commercial frequency domain diffraction code was used to obtain the inviscid hull forces [4]. Viscous forces on the hull were assumed negligible.

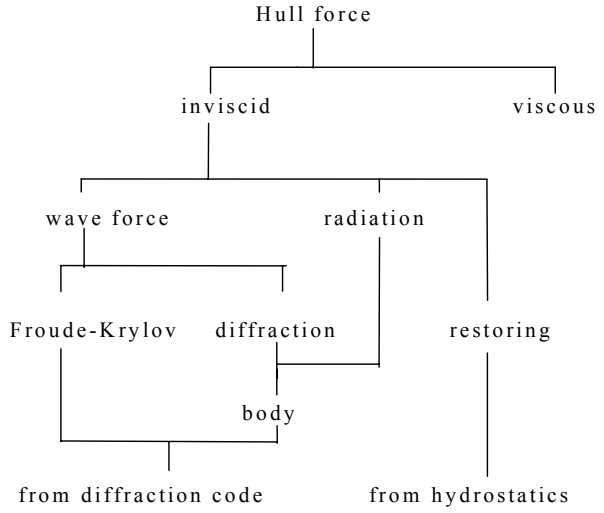

Figure 1 Hull force model

The force model for the water and air appendages is shown in Figure 2 below.

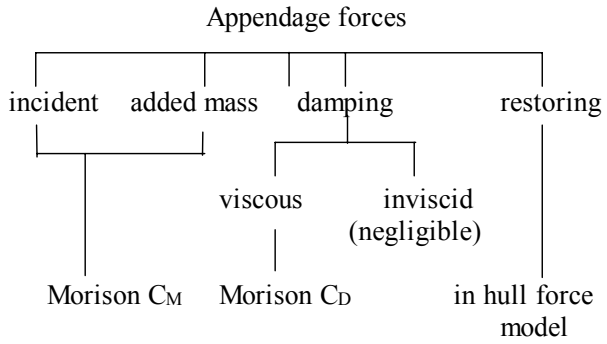

Figure 2 Appendage force model

The appendages were assumed to be small with respect to wavelength and deeply submerged, thus exhibiting negligible free surface effects, so a stripwise (horizontal segments) Morison treatment was used.

$$f = C_M \rho \frac{\pi}{4} D^2 \dot{u} - (C_M - 1)\rho \frac{\pi}{4} D^2 \ddot{x}$$

$$+ C_D \frac{\rho}{2} D|u - \dot{x}|(u - \dot{x}) \qquad (1)$$

where
f = force per strip
C_M = inertia coefficient
C_D = drag coefficient
D = representative length (chord for a foil)
u = instantaneous local fluid particle velocity
x = instantaneous local sway
ρ = fluid density

Note that u, x and D are functions of distance below the waterline. The inertia and drag coefficients [5] were determined empirically. They are functions of both Keulegan-Carpenter (KC) and Reynolds (Rn) numbers where

$$KC = \frac{UT}{D} \qquad (2)$$

$$Rn = \frac{UD}{\nu} \qquad (3)$$

where
U = relative velocity amplitude
T = period of oscillation
D = strip length
ν = kinematic viscosity

Typical KC values for the appendages ranged from 0 to 10, with Rn of the order 10^3. An inertia coefficient of $C_M = KC^{0.5}$ was used in the model, with a lower limit of 1.5. This formula was derived from a number of sources e.g. [6]. The drag coefficient was given by:

$$C_D = 8KC^{-0.333} \qquad (4)$$

from [7]), with a C_D upper limit of 8. This was derived from experimental data on flat plates at KC<10. Reynolds number dependence was not accounted for in the model.

The presence of a free-stream flow (ocean current or wind) will usually result in the flow direction shifting away from the surface normal direction assumed for the coefficients used in the Morison equation. Under such circumstances the appendage is operating as a foil at an angle of attack. There is a dearth of experimental data for foils in oscillating flow over the full range of attack angles. Even for steady flow, available data are limited. The side force generated by free stream flow over the appendages was included as an additional force term in the Morison equation. The calculation was based on low aspect ratio airfoil theory in steady flow for inflow angles less than 20 degrees. A larger inflow angle implies both stalled flow and a low ratio of flow speed to sway velocity. In such circumstances the flow speed effect is often likely to be small, so was ignored.
The oscillation of the flow vector over a roll cycle will also influence the force generated. A phase lag was introduced to simulate this effect.

Full Scale Trials

Two types of full scale experiment were conducted – free roll decay tests and irregular wave tests. The vessel used was a 10m sailing yacht. Motions were recorded for the free roll decay tests with and without the mainsail hoisted, in very light winds. Linear analysis of the roll decay tests was conducted to yield damping ratios β, where

$$\beta = \frac{b}{2\sqrt{ac}} \qquad (5)$$

in the single degree of freedom equation

$$a\ddot{\varphi} + b\dot{\varphi} + c\varphi = 0 \qquad (6)$$

where
φ = roll angle

The irregular wave tests were conducted again in very light winds with the vessel anchored with and without the mainsail hoisted, for a range of wave headings. Wave direction was altered by roping the vessel across the waves. Wave amplitude and frequency were measured by an accelerometer-based wave buoy lightly tethered to, and approximately one boat length downwind from the yacht. The wave energy during the experiments was very low and the load on the anchor cable was negligible

The roll Response Amplitude Operator (RAO) did not show any clear change with vessel heading varying from 90 to 150 degrees, so a further set of trials was conducted to measure roll and yaw on the yacht anchored in waves. The time series was analysed by dividing it up into segments of at least 10 seconds duration on the criterion that the yaw angle lay within a predetermined 5 degree bin for that segment duration. The rms roll angle and mean yaw angle were then calculated for each segment. The results showed very little correlation of rms roll angle with yaw angle (see Figure 3.)

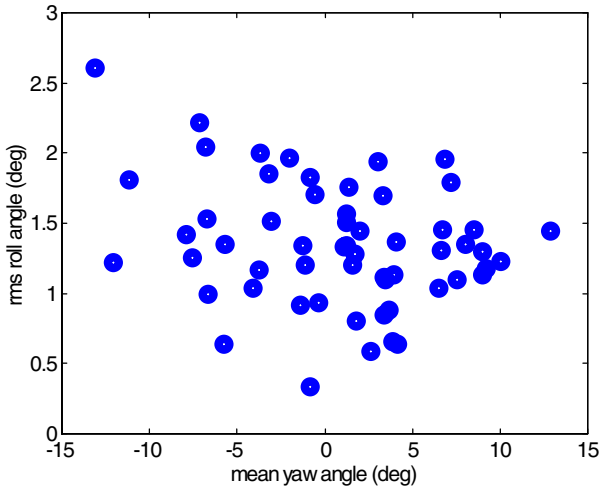

Figure 3 Scatter plot of rms roll v. yaw.

Results and Discussion

The most immediately apparent result from the numerical model was the effect of appendage damping. Figure 4 shows the effect of appendages on roll response, where

μ = wave direction relative to stern seas

W = non - dimensional frequency

$$= \omega\sqrt{\frac{B}{g}} \qquad (7)$$

ω = wave radial frequency

B = waterline beam = 2.88m

g = acceleration due to gravity

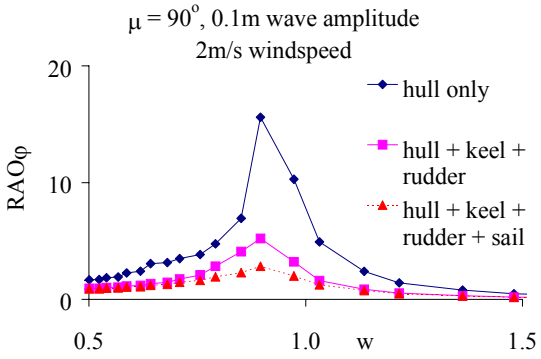

Figure 4 Effect of appendages

It was evident that the keel and rudder provided far greater damping than the hull, and that the sail was similarly effective. It is possible that the keel and rudder provide even more damping than calculated, as free surface effects were not included. Figure 5 below shows there was a significant degree of non-linearity when the damping was restricted to hydrodynamic sources.

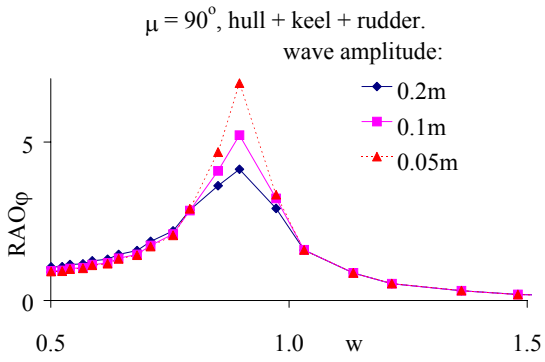

Figure *5* Effect of wave amplitude - no sail

However, the non-linearity of the overall system was considerably reduced when the sail was included, its dominating contribution to the damping being independent of wave amplitude. If the model was run without appendages, the response was almost linear, the weak non-linearity of the restoring coefficient being the only anomaly.

Figure 6 shows the importance of wind speed in generating sail damping, for a head wind.

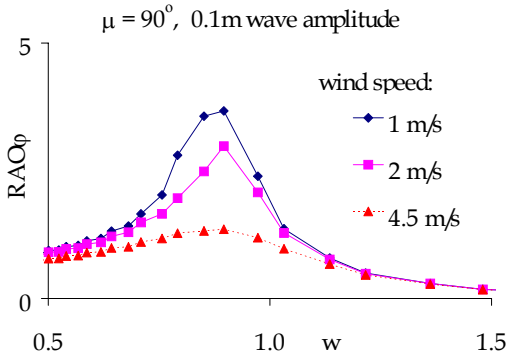

Figure 6 Effect of wind speed on sail damping

A variation of just 1m/s reduced the peak roll response by 20%. If it were possible to anchor with the sail up in a modest 4.5m/s wind, the roll amplification could be virtually eliminated. Similar results were found for ocean current effects on the keel and rudder.

Examples of full scale and simulated time series for the free decay tests are shown in Figure 7. The natural periods showed very good agreement but there were discrepancies in the roll decay.

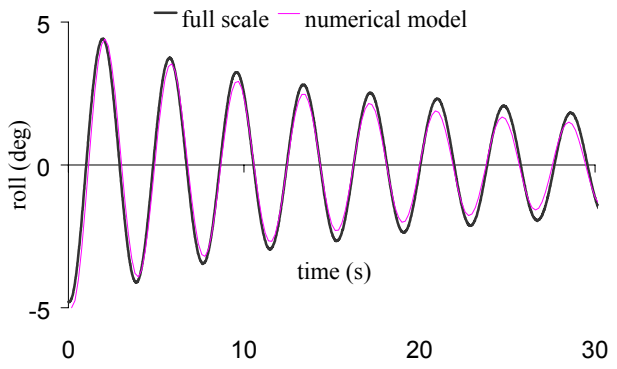

Figure 7 Comparison with full scale roll decay tests - no sail

The roll period of 3.8 seconds did not change significantly with the hoisting of the mainsail, and was very similar to the peak roll response frequency in the irregular wave tests.

The effect of the mainsail on the roll damping was very large, and similar in magnitude for both the free decay and irregular wave tests. The damping ratios β from the full scale free decay tests were 0.025 and for 0.079 mainsail stowed and mainsail hoisted respectively. This was comparable with the effect seen in both the numerical model and the full scale trials in waves.

Comparison with the full scale trials results in irregular waves was difficult because of the non-linear response with respect to wave amplitude. It was not possible to determine accurately the phasing between wave surface elevation and motion, so the RAO was determined from the wave spectrum rather than the time series. The amplitudes of the frequency components in a spectrum are not unique - they depend on the number of components used - so the wave amplitude of each frequency cannot be defined uniquely. The numerical model only accepts sinusoidal input so a 0.1m wave amplitude was chosen for comparisons, based on visual observations during the full scale trials (see Figure 8).

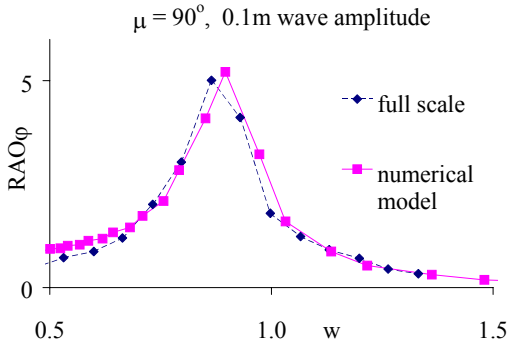

Figure 8 Comparison of numerical model with full scale wave trials - 90 deg wave heading, no sail

The model and trials response at oblique wave heading (Figure 9) did not agree nearly as well as for the beam sea condition (Figure 8). A likely source of discrepancy was the directional spread of waves at full scale. This had the effect of smearing any directional dependency. The combined results of figures 7, 8 and 9 imply that the numerical model overestimated the damping.

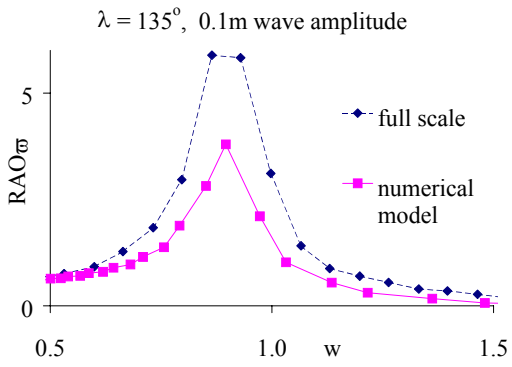

Figure 9 Comparison with full scale wave trials - 135 deg wave heading, no sail

Conclusions and Recommendations for Further Work

The numerical model developed has proved to be a useful investigative tool. It has not yet been possible to conduct extensive validation, but comparison with full scale trials showed good general agreement. The results showed that:

- appendages formed the bulk of the damping sources;
- the effect of the sail on damping was very noticeable, particularly in a wind field;
- the hydrodynamic damping was non-linear with respect to wave amplitude;
- the model predicted a strong influence of wave heading on roll motion, which was not borne out by the full scale trials.

The next stage of research is to conduct a series of scale model tests in regular waves. A hull form with minimal damping will be used to attach appendages of various types. This will provide a data set for validation of the numerical model. The level of agreement between the code and the experimental data will determine the next step. If agreement is good, the model will be extended to include motion coupling and shallow water effects, backed up by further model tests - possibly forced oscillations in calm water.

References

[1] A. Lloyd, *Seakeeping: ship behaviour in rough weather*. Chichester: Ellis Horwood, 1989.

[2] N. J. Newman, *Marine hydrodynamics*. Cambridge Massachusetts: MIT Press, 1977.

[3] O. M. Faltinsen, *Sea loads on ships and offshore structures*. Cambridge: Cambridge University Press, 1990.

[4] MIT, "WAMIT. A Radiation-Diffraction Panel Program for Wave-body Interactions," , 5.3 ed: MIT, 1995.

[5] G. H. Keulegan and L. H. Carpenter, "Forces on cylinders and plates in an oscillating fluid," *Journal of Research of the National Bureau of Standards*, vol. 60, pp. 423-440, 1958.

[6] T. Sarpkaya and J. L. O'Keefe, "Oscillating flow about two- and three-dimensional bilge keels," presented at 14th International Conference on Offshore Mechanics and Arctic Engineering, Copenhagen, 1995.

[7] J. M. R. Graham, "The forces on sharp-edged cylinders in oscillatory flow at low Keulegan-Carpenter numbers," *Journal of Fluid Mechanics*, vol. 97, pp. 331-346, 1980.